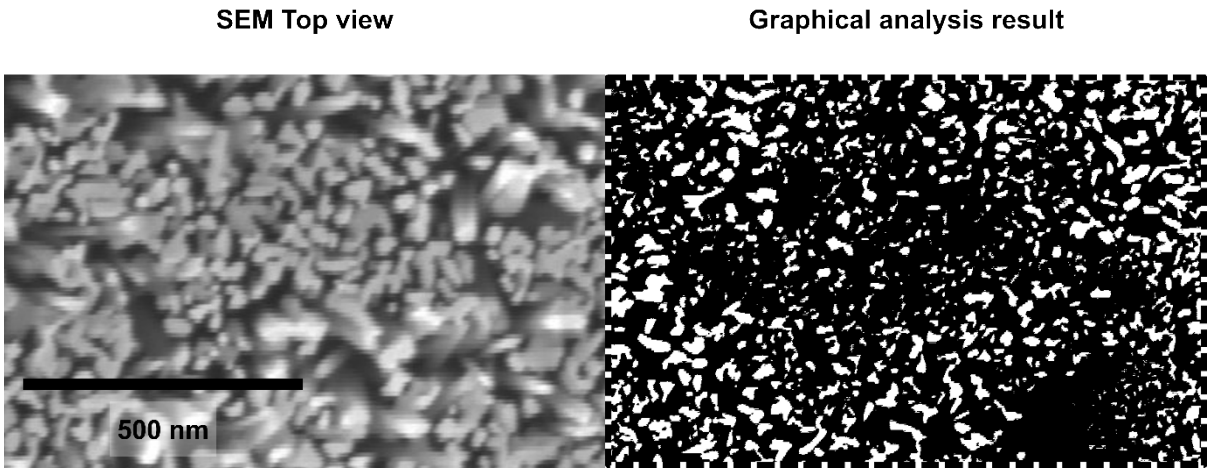

Figure S1. SEM image of GaN NRs

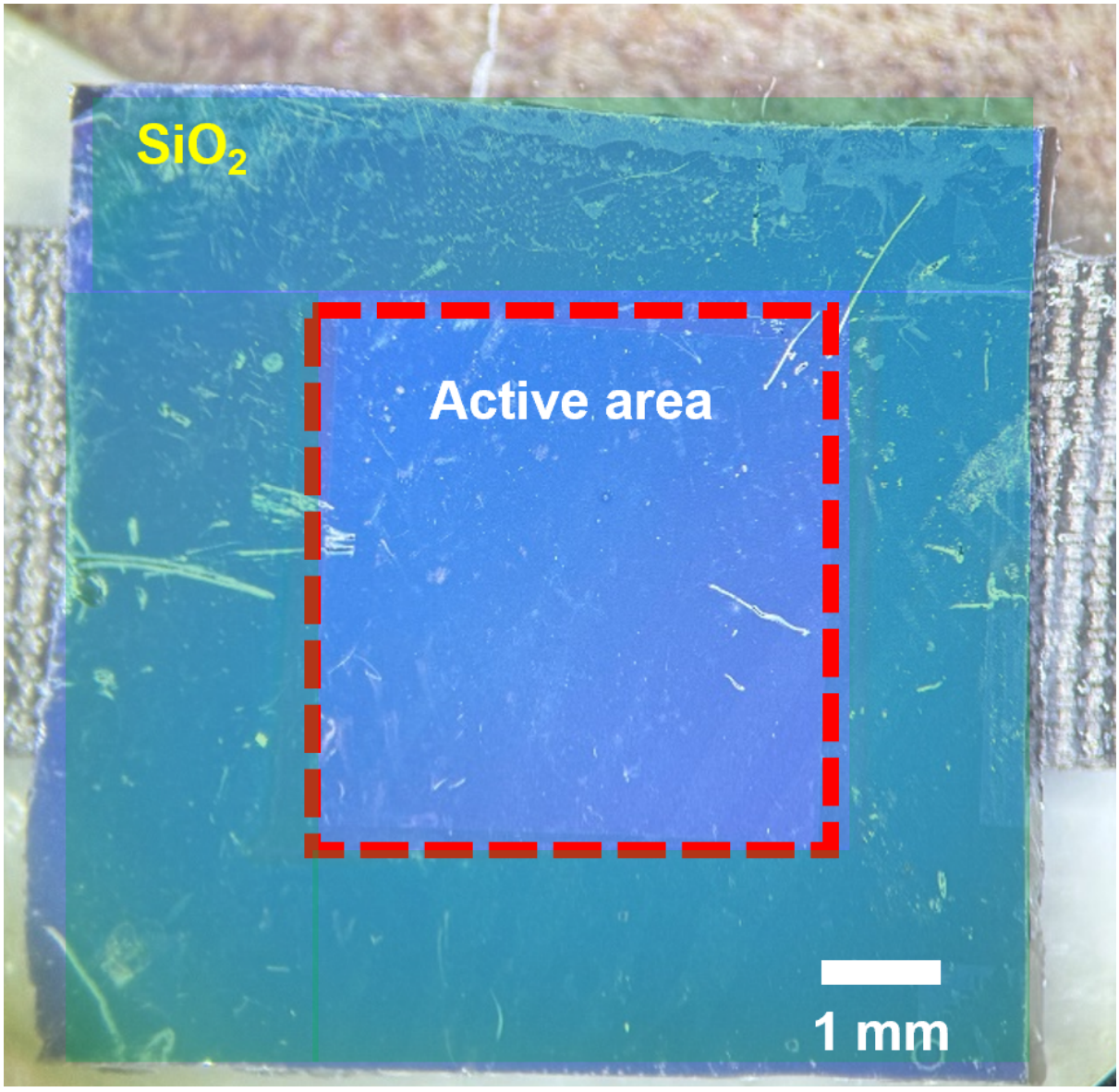

Figure S2 Photograph of the fabricated SH-PD.

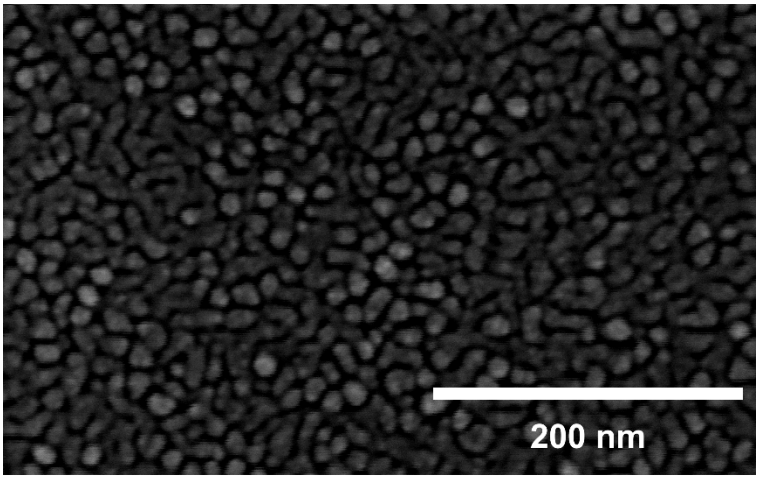

Figure S3 FE-SEM image of ZTN thin film

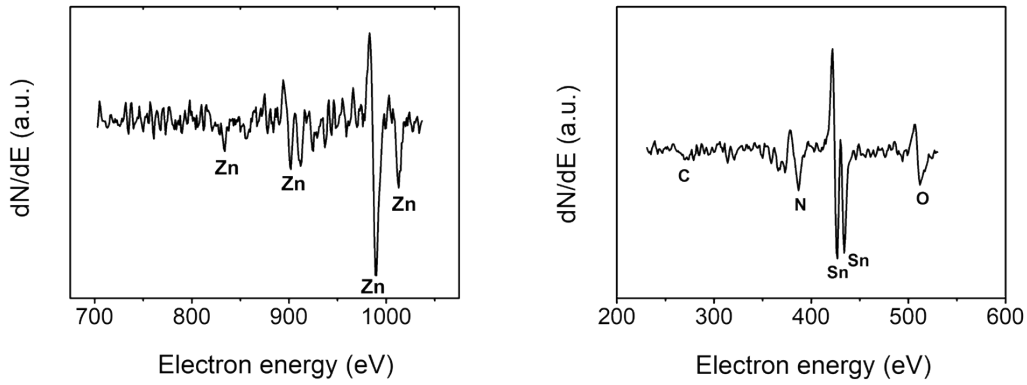

Figure S4 AES results of ZTN thin film

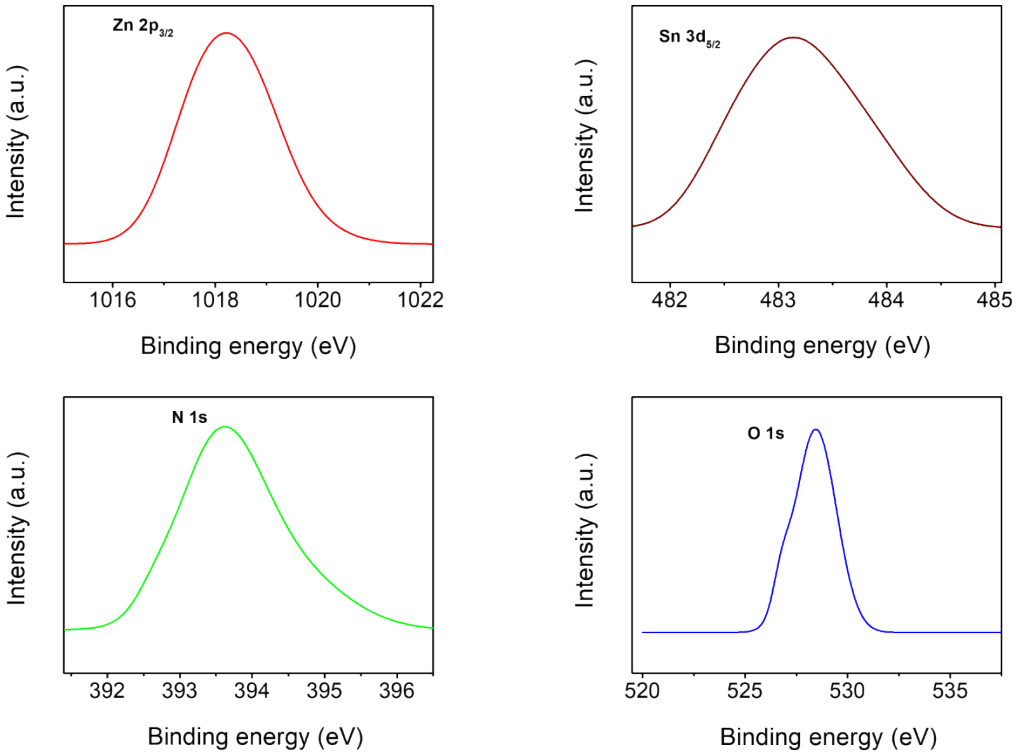

Figure S5 XPS results of ZTN thin film

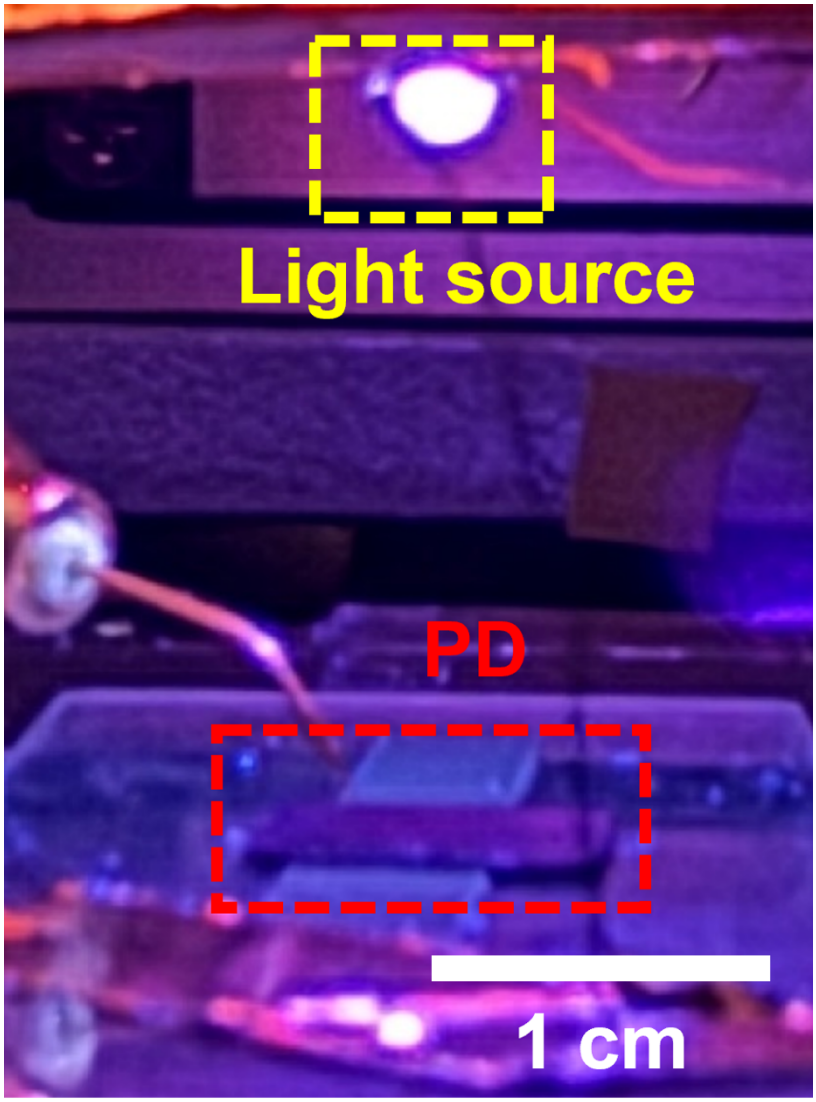

Figure S6 Experimental set-up for measuring optical/electrical properties of the devices.

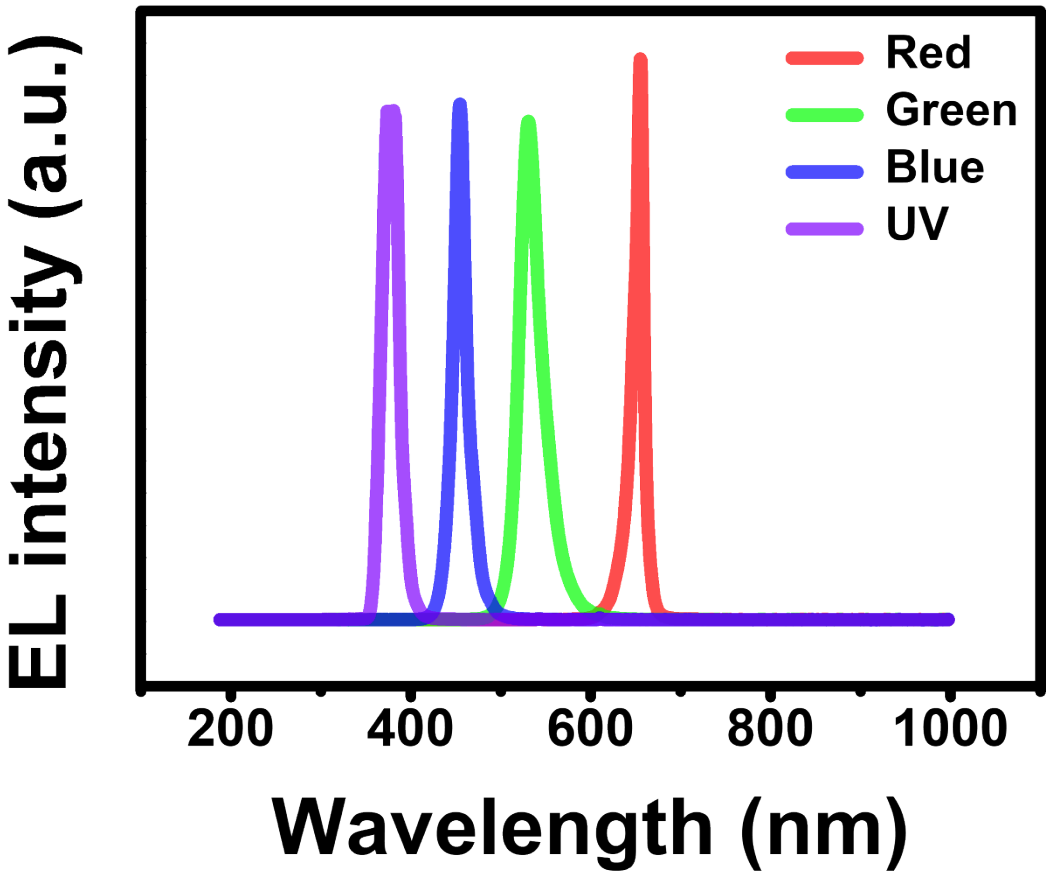

Figure S7 EL spectrum of the conventional light sources (UV, blue, green and red light).

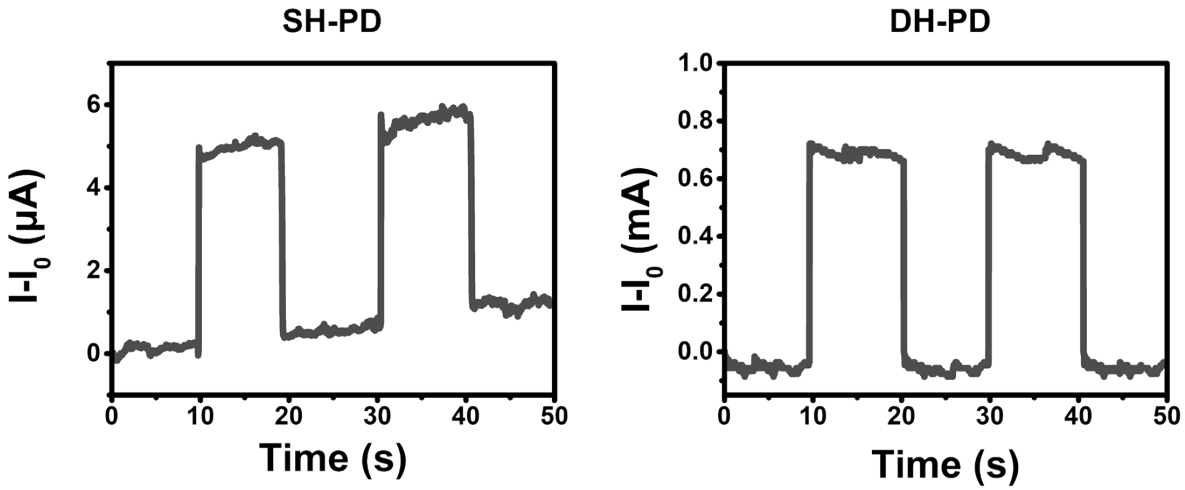

Figure S8 Operation testing results of SH-PD (left) and DH-PD (right)

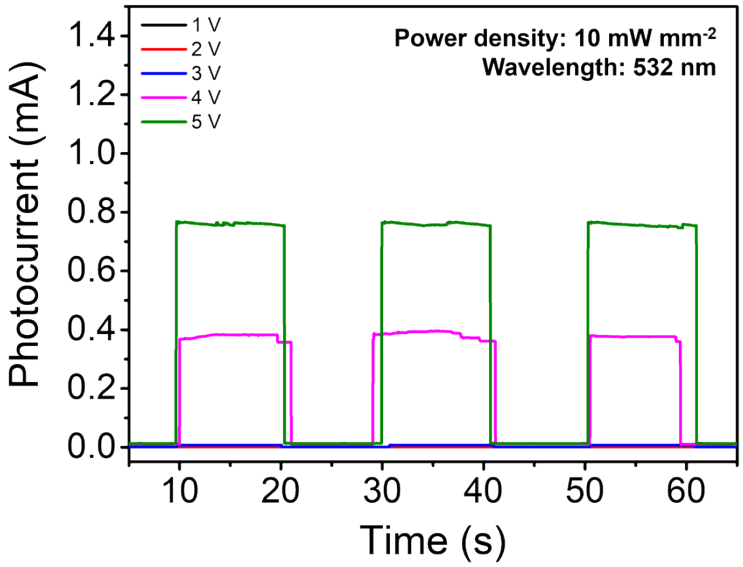

Figure S9 Voltage-dependent device operation test

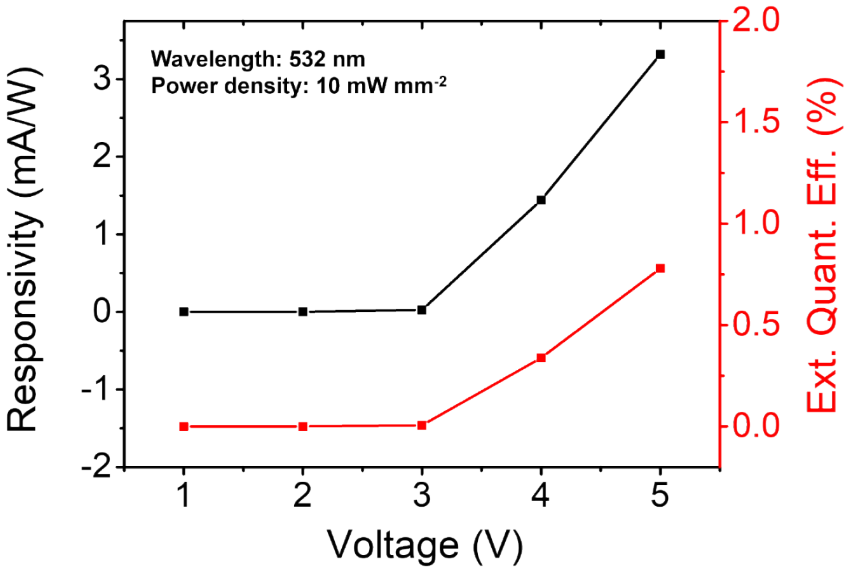

Figure S10 R and EQE value of voltage-dependent on/off test

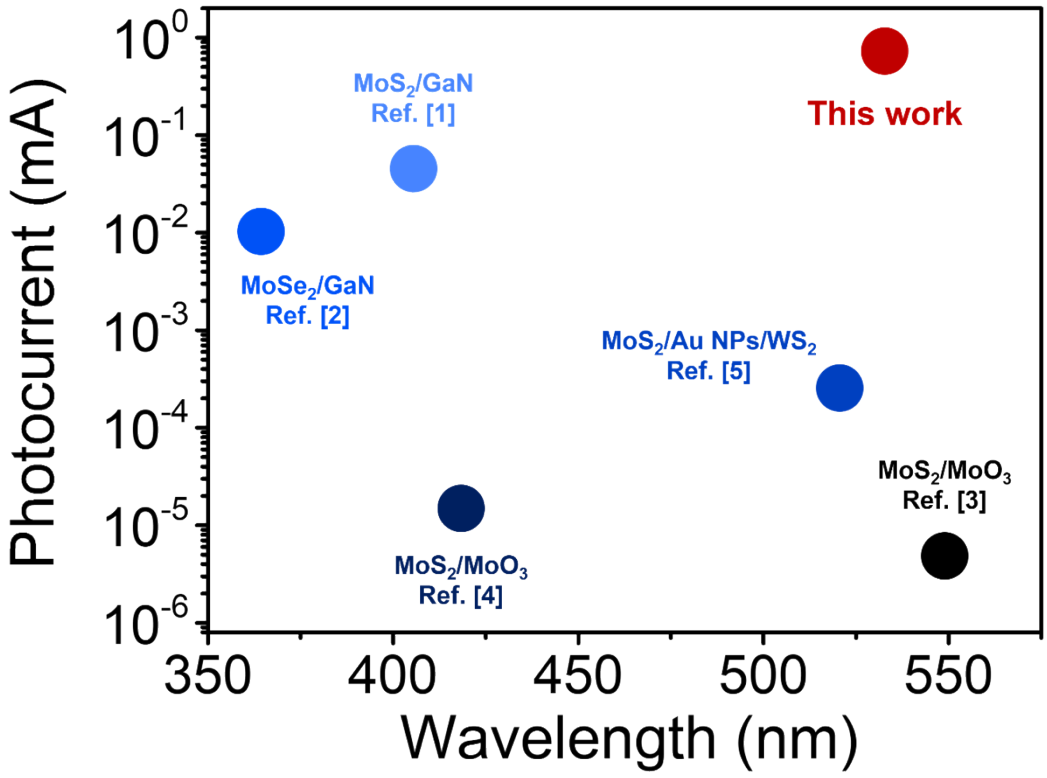

Figure S11. The performance comparison result of reported heterojunction-based PDs

	thickness [nm]	Bulk concentration N_b [cm^{-3}]	Mobility μ [$cm^2 V^{-1}s^{-1}$]
ZTN thin film	242.1	-2.39E+19	1.33E+01

Table S1 Bulk carrier concentration and mobility of ZTN thin-film

Voltage	Photocurrent	Dark current	Responsivity	EQE
1 V	0.504 μA	0.315 μA	0.759 μA/W	1.78×10^{-4}%
2 V	1.020 μA	0.572 μA	1.81 μA/W	4.25×10^{-4}%
3 V	7.341 μA	1.000 μA	25.3 μA/W	5.95×10^{-3}%
4 V	37.14 μA	10.81 μA	1.44 mA/W	3.38×10^{-1}%
5 V	733.7 μA	13.46 μA	3.32 mA/W	7.79×10^{-1}%

Table S2 Summary of voltage-dependent on/off test

Material	Photocurrent	Dark current	Wavelength	ΔI	Ref
MoS_2/GaN	40.5 μA	0.2 μA	405 nm	40.3 μA	[1]
$MoSe_2$/GaN	10.5 μA	0.95 μA	365 nm	9.55 μA	[2]
MoS_2/MoO_3	4.7 nA	1.3 pA	550 nm	4.7 nA	[3]
MoS_2/MoO_3	15.56 nA	6 pA	420 nm	15.56 nA	[4]
MoS_2/Au NPs/WS_2	230 nA	1.1 pA	520 nm	230 nA	[5]
ZTN/GaN/Si	733 μA	13 μA	532 nm	720 μA	This work

Table S3 The photocurrent, dark current and wavelength comparison result of reported heterojunction-based PDs

1 M. Moun, M. Kumar, M. Garg, R. Pathak, and R. Singh, Understanding of MoS_2/GaN Heterojunction Diode and its Photodetection Properties, *Sci. Rep.*, 2018, **8**, 11799.

2 H. K. Sandhu, J. W. John, A. Jakhar, A. Sharma, A. Jain, and S. Das, $MoSe_2$/n-GaN Heterojunction Induced High Photoconductive Gain for Low-Noise Broadband Photodetection from Ultraviolet to Near-Infrared Wavelengths, *Adv. Mater. Interfaces.*, 2022, **9**, 2102200.

3 H. Li, T. Zhang, Z. Yi, X. Chen, Z. Dai, and J. Tan, High Sensitive and Stable UV–Vis Photodetector Based on MoS_2/MoO_3 vdW Heterojunction, *ACS Appl. Mater. Interfaces*, 2024, **16**, 33829-33837.

4 R. Singh, M. Kumar, U. Kim, and H. Seo, Self-Powered and High-Performance Alternating Current Photodetectors to enhance Broadband Photodetection, *Adv. Electron. Mater.*, 2022, **8**, 2200392.

5 Z. Lin, P. Luo, W. Zeng, H. Lai, W. Xie, W. Deng, and Z. Luo, Improvement of photoelectric properties of MoS_2/WS_2 heterostructure photodetector with interlayer of Au nanoparticles, *Opt. Mater.*, 2020, **108**, 110191.